



Optical MIMO: Results and analysis

Apostolos Karadimitrakis, Merouane Debbah, Aris Moustakas

► To cite this version:

Apostolos Karadimitrakis, Merouane Debbah, Aris Moustakas. Optical MIMO: Results and analysis. 11th International Symposium on Wireless Communication Systems (ISWCS), Aug 2014, Barcelona, Spain. pp.966 - 970, 10.1109/ISWCS.2014.6933493 . hal-01098894

HAL Id: hal-01098894

<https://hal.science/hal-01098894>

Submitted on 17 Jan 2015

HAL is a multi-disciplinary open access archive for the deposit and dissemination of scientific research documents, whether they are published or not. The documents may come from teaching and research institutions in France or abroad, or from public or private research centers.

L'archive ouverte pluridisciplinaire **HAL**, est destinée au dépôt et à la diffusion de documents scientifiques de niveau recherche, publiés ou non, émanant des établissements d'enseignement et de recherche français ou étrangers, des laboratoires publics ou privés.

Optical MIMO: Results and Analysis

Apostolos Karadimitrakakis^{1,2}, Merouane Debbah² and Aris L. Moustakas^{1,2}

Abstract—Spatial Division Multiplexing (SDM) is being increasingly applied to optical fiber systems [1]. Thus, SDM is gradually becoming a fundamental part of modern telecommunications aiming to provide higher transmission rates that are both error-free and inexpensive. So far, engineers considered packing and operating the many different laser as the biggest problem, but as it seems, the crosstalking phenomenon between the various in-fiber propagating modes creates a great barrier, which needs sophisticated methods to overcome, such as MIMO techniques, which are well known in the wireless field. In this paper, we analyze real data from multimode optical fibers and find that crosstalk seems to be significant. If this is the case, the reception can be problematic without MIMO techniques.

Index Terms—Optical fiber transmission, MIMO, channel capacity, crosstalking

I. INTRODUCTION

SO far, wireless networks have seen an unprecedented growth, both in their deployment and in their traffic load to meet the increasing demand: In the past, consumers were mostly interested in voice and short message services, so 2G technology absolutely covered their needs. Today, internet browsing along with social network connectivity and real-time navigation is provided by 3G and early 4G. For the future 5G, or even smart handover of service between different technologies i.e. SDR (*Software Defined Radio*) are being researched to accommodate new services like high definition voice, video streaming and DVB-T. Atop all these, devices themselves will be connected to internet exchanging information, forming the so-called *internet of things*. In order to feed the ever hungry demand, optical backhaul networks are being deployed. These networks have an extremely vast bandwidth, but, contrary to the wireless development, the wired progress, has come to a halt. Thus, inevitably, we will face a most troubling problem: a capacity crunch between the wireless (end-user) network and the wired (backhaul) network [2].

In fact, we are already reaching the limits of the “classical” (SMF - *Single Mode Fiber*) fiber optic communications, which forces us to investigate new ways of better exploiting the corresponding bandwidth. For that, *Multi Core Fibers* (MCF) or *Few Mode Fibers* (FMF) have been developed, which along with the MMF (*Multi Mode Fibers*), allow the light to propagate using spatial division, thus increasing considerably the available channel capacity. An MMF, contrary to SMF, has a larger core diameter, which exceeds the wavelength of the propagating light. That characteristic allows the excitation

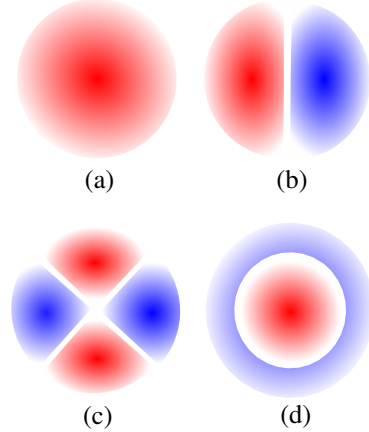


Fig. 1: Mode profiles of the lower-order fiber modes (a) LP_{01} (b) LP_{11} (c) LP_{21} (d) LP_{02}

of more than one propagation modes (see Fig. 1), but at the same time makes the communication system suffer from *modal dispersion* [3]. Moreover, as the number of transmitters increases, the crosstalk phenomenon occurs [4], [5]: In order to fit the many different propagating ways inside the constricted space of the fiber, the distance between these propagating modes has been reduced to a minimum, thus inevitably, they experience crosstalking with adjacent ones. In this paper we will show that the crosstalking phenomenon is present even for a 4×4 optical MIMO system of a very short span.

A. Outline

In Section II we present our optical MIMO model along with the equalization technique. In Section III we present our analysis and the various results. In Section IV we study the effect of noise on our channel estimation and propose an improved equalization technique. Finally, in Section V we conclude.

II. OPTICAL MIMO MODEL

A. Optical MIMO Channel

The equation of the optical MIMO channel as can be seen in Fig. 2 is

$$\mathbf{r} = \mathbf{C}\mathbf{s} + \mathbf{w}, \quad (1)$$

where \mathbf{s} , \mathbf{r} , \mathbf{w} is the input, output and Additive White Gaussian Noise Vector (AWGN) respectively, before the Fractionally Spaced Equalizer (FSE). \mathbf{C} is the channel matrix which is constructed by the coefficients of the different MIMO sub-channels. The output of the equalizer is, therefore,

$$\mathbf{y} = \mathbf{f}^T \mathbf{r} \quad (2)$$

(1): Department of Physics, University of Athens, Greece

(2): Alcatel-Lucent Chair, Gif-sur-Yvette, France

This research has been supported by the ERC Starting Grant 305123 MORE (Advanced Mathematical Tools for Complex Network Engineering) and the project HENIAC.

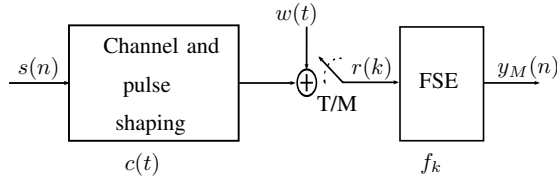


Fig. 2: Schematic representation of our system.

where \mathbf{f} is a vector constructed by the equalizer coefficients, used to “extract” the desired signal.

B. Realization

Our system consists of a very short piece of MMF fiber between MUX and DeMUX. 5 modes LP01, LP11 a+b and LP21 a+b being injected in the system (LP11 and LP21 have 2 polarizations, “a” and “b”), while the receiver reads LP21 a+b and processes them in parallel in a MIMO 4×4 adaptive (blind) equalizer driven by *Constant Modulus Algorithm* (CMA [6]. Each polarization is equally stimulated. At the receiver there are 4 equalizers, each one with 4 filters (see Fig. 3). Each filter consists of 25 taps because we need to recover not only the state of the polarization (or mode) which would be memoryless, but also to recover all the other impairments coming from the signal (*Intersymbol Interference- ISI*) or from the channel (chromatic dispersion and polarization/spatial-mode dispersion). The sequence used is $2^{15} - 1$ PRBS -*Pseudo Random Binary Sequence* of PDM-QPSK at a rate of 32 GBs. Each “Equalizer” variable is the state of the equalizer at the end of the processing of an acquisition. The scope is triggered every 5 seconds and an acquisition lasts 40ms. At the end of the processing of an acquisition we register the output of each of the 25 taps ($T/2$ spaced) of the 16 equalizer filters. In Fig. 2 we can see a representation of our system, where $s(n)$ is the PRBS sequence/signal, $c(t)$ is the channel, $w(t)$ is the AWGN, FSE is the *Fractionally Spaced Equalizer* with “equalizer” variables f_k and $y_M(n)$ is the signal after the equalizing processing. The multi-channel model of Fig. 4 subdivides the fractionally spaced channel coefficients $c_k = c(k\frac{T}{2})$ and the discrete-time random process $w_k = w(k\frac{T}{2})$ into even and odd counterparts, [6], so that $c_n^{even} = c_{2n}$ and $c_n^{odd} = c_{2n+1}$ for $n = 0, 1, \dots$. In an analogous way, the coefficients of the *Fractionally Spaced Equalizer* (FSE), \mathbf{f} , are partitioned as $f_n^{even} = f_{2n}$ and $f_n^{odd} = f_{2n+1}$. That way, we can create

$$\mathbf{C}_e = \begin{bmatrix} c_0^{even} & & & \\ c_1^{even} & c_0^{even} & & \\ \vdots & c_1^{even} & & \\ c_{M-1}^{even} & \vdots & c_0^{even} & \\ & c_{M-1}^{even} & c_1^{even} & \\ & & \vdots & c_{M-1}^{even} \end{bmatrix}, \quad \mathbf{C}_o = \begin{bmatrix} c_0^{odd} & & & \\ c_1^{odd} & c_0^{odd} & & \\ \vdots & c_1^{odd} & & \\ c_{M-1}^{odd} & \vdots & c_0^{odd} & \\ & c_{M-1}^{odd} & c_1^{odd} & \\ & & \vdots & c_{M-1}^{odd} \end{bmatrix}$$

which are matrices of size $P \times N$ where $P = M + N + 1$, M is the length of a counterpart of the channel coefficients and N , analogously, is the length of a counterpart of FSE coefficients. The impulse response, \mathbf{h} , of the linear system relating s_n to

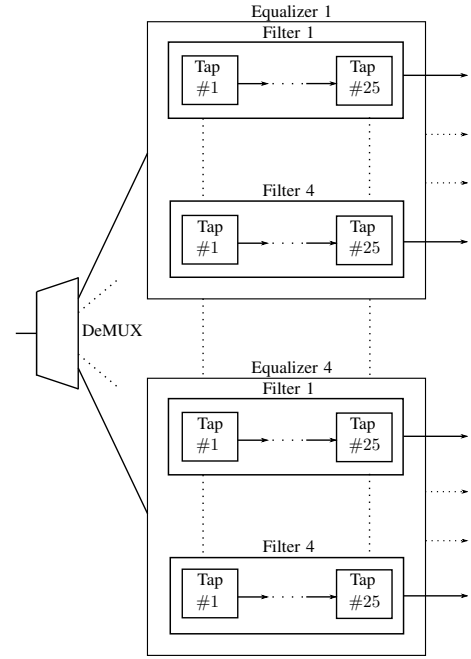


Fig. 3: Block schema of the receiver

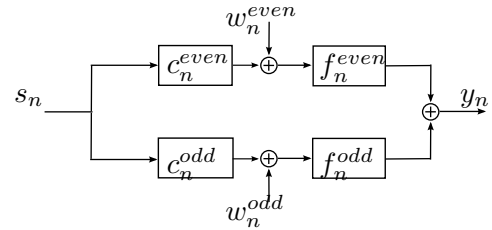


Fig. 4: Multi-channel paradigm, subdivided into odd and even counterparts.

y_n can be constructed so that

$$\mathbf{h} = \mathbf{C}\mathbf{f}, \quad (3)$$

where $\mathbf{C} = [\mathbf{C}_o \ \mathbf{C}_e]$ and $\mathbf{f}^T = [\mathbf{f}_e \ \mathbf{f}_o]$. In case of perfect equalization and *Perfect Source Recovery* (PSR) it is $\mathbf{h}_\delta = [0, 0, \dots, 1, \dots, 0]$, where the non-zero coefficient is in the δ th position ($0 \leq \delta \leq P - 1$). For PSR under arbitrary δ , \mathbf{C} must be of full row rank [7]. To simplify our notation we can construct the matrix \mathbf{C}_{FS} of size $(M + N) \times 2N$ from a vector of fractionally-spaced channel coefficients $\mathbf{c}_{FS} = [c_0, c_1, \dots, c_{2M-1}]^T$ so as

$$\mathbf{C}_{FS} = \begin{bmatrix} c_0 & & & & & \\ & c_0 & & & & \\ & c_1 & & & & \\ & \vdots & & & & \\ c_{2M-1} & \vdots & \ddots & & c_0 & \\ & c_{2M-1} & & & c_1 & \\ 0 & & & & \vdots & \\ & & & & & c_{2M-1} \end{bmatrix}, \quad (4)$$

and the full rank requirement dictates that

$$2N \geq M + (N - 1) \Rightarrow N \geq M - 1. \quad (5)$$

Finally, the n th equalizer output can be written as

$$y_n = \mathbf{s}^t(n)\mathbf{C}\mathbf{f} + \mathbf{w}^t(n)\mathbf{f}. \quad (6)$$

C. Methodology

As was stated in the beginning, we have acquired and saved the equalizer coefficients \mathbf{f}_{2N} . Our aim is to compute the channel coefficients \mathbf{c}_{2M} only by using the already known \mathbf{f}_{2N} . In the case of PSR, we know that $\mathbf{h}_\delta = \mathbf{C}\mathbf{f}$, therefore for our real data it is a classic problem of finding \mathbf{C} while minimizing the squared ℓ_2 norm :

$$\|\mathbf{C}\mathbf{f} - \mathbf{h}_\delta\|_2^2 = \|\mathbf{C}\mathbf{f}\|_2^2 - 2\mathbf{h}_\delta^T\mathbf{C}\mathbf{f} + 1, \quad (7)$$

which is a quadratic equation of the form $\mathbf{c}^T\mathbf{A}\mathbf{c} - 2\mathbf{c}^T\mathbf{v}$, where \mathbf{A} is the quadratic part and \mathbf{v} is the linear part. To minimize (7), we take the derivative with respect to \mathbf{c} and set it to zero, which solves for

$$\mathbf{c} = \mathbf{A}^{-1}\mathbf{v}. \quad (8)$$

We can take advantage of the toeplitz characteristics of \mathbf{C} and write (7) analytically,

$$\begin{aligned} & \sum_{m=0}^{2M-1} \sum_{m'=0}^{2M-1} c_m c_{m'} \sum_{k_{\max}(m, m')}^{2N-1+\min(m, m')} f_{k-m} f_{k-m'} \\ & - 2 \sum_{l=\max(0, \delta-2M)}^{\min(2N-1, \delta)} c_{\delta-l} f_l + 1 = 0. \end{aligned} \quad (9)$$

III. REAL DATA ANALYSIS AND RESULTS

As a first step in our data analysis, we plot the average of the output of the filter taps; see Fig. 5. We can distinguish that for every equalizer, there is a dominant filter, which has a maximum at almost the same tap, the 13th. It has to be mentioned though that although the averaged output has always maximum at the 13th tap, this is not the general rule for every instantiation. That characteristic, gives us the hint of $\delta = \# \max(f_{2N})$. In fact, we check our hypothesis: $\min(\|\mathbf{C}\mathbf{f} - \mathbf{h}_\delta\|)$ and it holds true, the proof of which is omitted. That way, we compute the \mathbf{c}_{2M} , for every equalizer, see Fig. 6. The number of spatial sub-channels M is set manually to $M = 9$. The reason for that is twofold: In the second part of (9) the argument of c is $\delta - l$ but the length of \mathbf{c} is $2M$. Therefore $2M \geq \delta - l \Rightarrow M_{\min} = \frac{\delta-l}{2}$. Moreover, we chose $M = M_{\min} = 9$ for computational simplicity.

In Fig. 7 we compute the CDF of the eigenvalues for different channel coefficients. By setting also the off-diagonal elements of the channel coefficients to zero, we plot 2 different group of curves, each one distinguished by the red and blue color. That way, the red color indicates there is no crosstalking in our system. Therefore, it is easily visible that our system suffers from cross-talking.

Finally, in Fig.8 we plot the MIMO channel capacity c_f for the different frequencies, with and without crosstalk.

$$c_f = \frac{1}{18} \sum_{f=1}^{18} \log \det(\mathbf{I}_4 + \rho \mathbf{H}^\dagger(f) \mathbf{H}(f)) \quad (10)$$

It is obvious that, by exploiting the MIMO gains, the channel capacity can be enhanced.

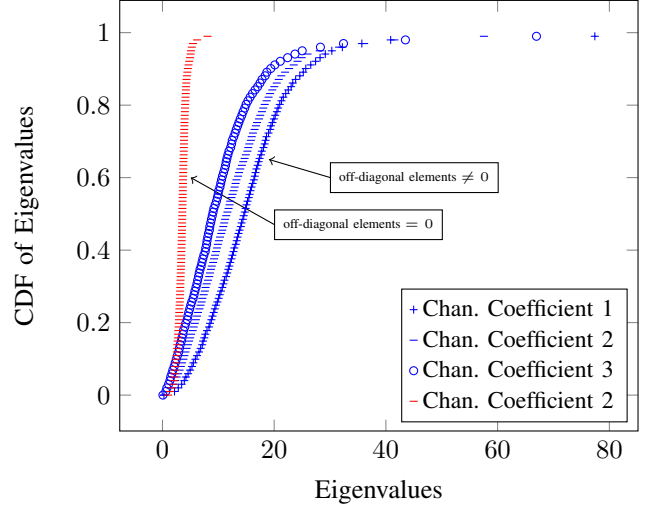


Fig. 7: CDF of eigenvalues for some channel coefficients.

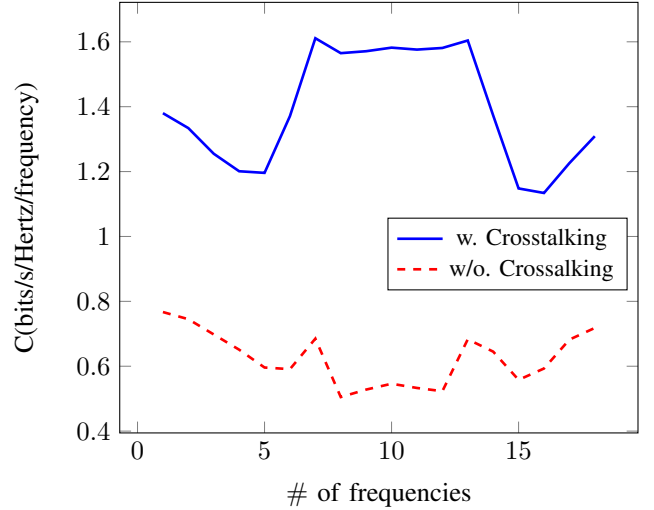


Fig. 8: Average capacity c_f for the different frequencies f , over the 500 instantiations.

IV. EFFECT OF NOISE ON CHANNEL ESTIMATION

In our experiment we registered only the equalizer coefficients, which left us uninformed about the noise, its characteristics and how it affects our proposed method of extracting the channel state information. To test the robustness of our algorithm, we construct a single pseudo-channel with coefficients \mathbf{c}_{2M} , $|\mathbf{C}_{2M}^2|^2 = 1$. The channel vector \mathbf{c} is sparse, with 7 non-zero elements and 11 zero ones. Channel matrix \mathbf{C} with dimensions $(M + N) \times 2N$ is constructed according to (4) with toeplitz characteristics, where $2N$ is the size of the equalizer vector \mathbf{f} . In order to ease our computations we set

$M = N$, thus \mathbf{C} is easily invertible. Arbitrarily we set $\delta = 7$. So, the estimated \mathbf{f}_{est} , without the presence of AWGN is

$$\mathbf{f}_{est}^T = \mathbf{C}^{-1}\mathbf{h}, \quad (11)$$

and reversely using the methodology from the previous section to estimate the channel coefficients \mathbf{c}_{est} , we end up in \mathbf{A}_{est} and \mathbf{V}_{est} .

1) *Sparse Channel Estimation*: In the case of noise presence, by considering our channel as sparse, we can estimate a new de-noised $\tilde{\mathbf{c}}_{est}$ by using a *Compressed Sensing* (CS) method based on *Dantzig Selector* (DS) [9]. Let us remember (8). By adding AWGN (\mathbf{z}), we get

$$\mathbf{c}_{noise} = \mathbf{A}^{-1}\mathbf{v} + \mathbf{z}. \quad (12)$$

\mathbf{v} is the solution to the following optimization

$$\min_{\tilde{\mathbf{v}}} \|\tilde{\mathbf{v}}\|_1 \text{ s.t. } \|\mathbf{A}^H(\mathbf{c} - \mathbf{A}^{-1}\tilde{\mathbf{v}})\|_\infty \leq \epsilon, \quad (13)$$

where $\tilde{\mathbf{v}}$ is the estimate of \mathbf{v} and ϵ is a constant, depending on the noise and the channel. In our case we set $\epsilon = 5 \cdot 10^{-3}$ As

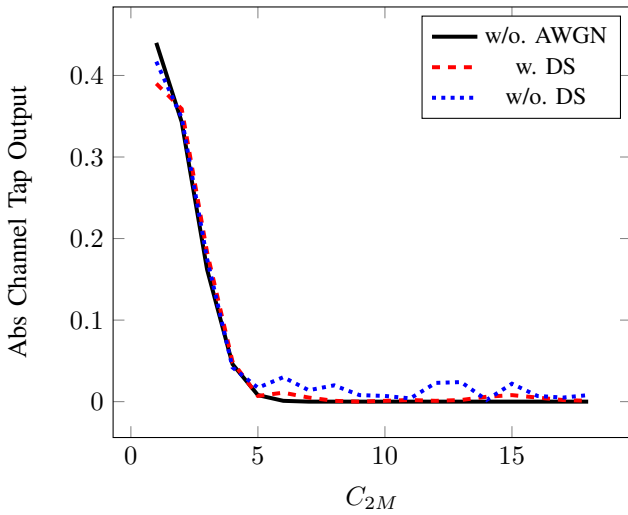


Fig. 9: Sparse channel coefficient estimation for $P_{noise} = -20dB$ per sample with and without the use of DS.

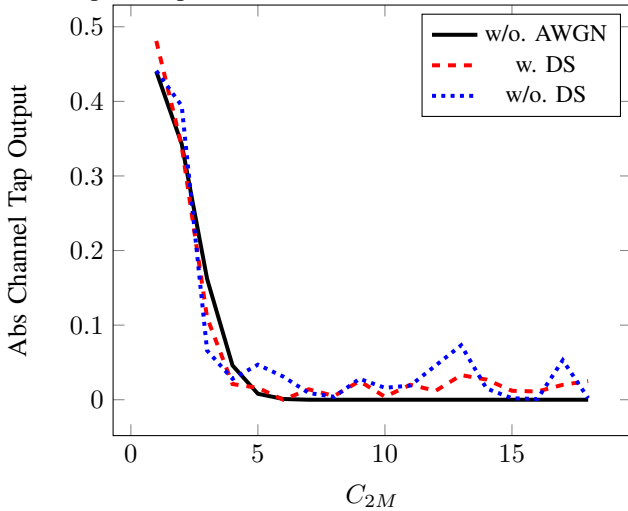


Fig. 10: Sparse channel coefficient estimation for $P_{noise} = -10dB$ per sample with and without the use of BPDN.

can be seen in Fig. 9, AWGN, can insert significant distortion in channel estimation. But on the other hand by using a CS algorithm like DS, the distortion can be minimized. The recreation of the channel is less effective for higher P_{noise} but yet the CS method shows significant effectiveness.

V. CONCLUSION

In [10], we have proven theoretically, that crosstalking is an existing impairment in fiber optic communications which incorporate SDM techniques. In this paper we showed that fiber optics is another field where MIMO techniques can find great usage. Moreover, due to the sparse characteristics of the channel, CS methods can further enhance the equalization process. A more realistic, practical implementation of an optical MIMO system along with a CS-equalization technique is a question for future work.

REFERENCES

- [1] R. Ryf, M. A. Mestre, S. Randel, X. Palou, A. H. Gnauck, R. Delbue, P. Pupaiaikis, A. Sureka, Y. Sun, X. Jiang, and R. Lingle, "Combined sdm and wdm transmission over 700-km few-mode fiber," in *Optical Fiber Communication Conference/National Fiber Optic Engineers Conference 2013*. Optical Society of America, 2013, p. OW11.2. [Online]. Available: <http://www.opticsinfobase.org/abstract.cfm?URI=OFC-2013-OW11.2>
- [2] D. J. Richardson, "Filling the light pipe," *Science*, vol. 330, no. 6002, pp. 327–328, 2010. [Online]. Available: <http://www.sciencemag.org/content/330/6002/327.short>
- [3] A. Gholami, D. Molin, and P. Sillard, "Compensation of chromatic dispersion by modal dispersion in mmf- and vcsel-based gigabit ethernet transmissions," *Photonics Technology Letters, IEEE*, vol. 21, no. 10, pp. 645–647, May 2009.
- [4] K.-P. Ho and J. M. Kahn, "Statistics of group delays in multimode fiber with strong mode coupling," *J. Lightwave Technol.*, vol. 29, no. 21, pp. 3119–3128, Nov 2011. [Online]. Available: <http://jlt.osa.org/abstract.cfm?URI=jlt-29-21-3119>
- [5] K.-P. Ho and J. Kahn, "Delay-spread distribution for multimode fiber with strong mode coupling," *Photonics Technology Letters, IEEE*, vol. 24, no. 21, pp. 1906–1909, Nov 2012.
- [6] J. Johnson, R. P. Schniter, T. Endres, J. Behm, D. Brown, and R. Casas, "Blind equalization using the constant modulus criterion: a review," *Proceedings of the IEEE*, vol. 86, no. 10, pp. 1927–1950, Oct 1998.
- [7] L. Tong, G. Xu, T. Kailath, and F. Ilee, "Blind identification and equalization based on second-order statistics: A time domain approach," *IEEE Trans. Inform. Theory*, vol. 40, pp. 340–349, 1994.
- [8] G. Gui, Q. Wan, S. Qin, and A. min Huang, "Sparse multipath channel estimation using ds algorithm in wideband communication systems," in *Image and Signal Processing (CISP), 2010 3rd International Congress on*, vol. 9, Oct 2010, pp. 4450–4453.
- [9] E. Candes and T. Tao, "The dantzig selector: Statistical estimation when p is much larger than n," *The Annals of Statistics*, vol. 35, no. 6, pp. 2313–2351, 12 2007. [Online]. Available: <http://dx.doi.org/10.1214/009053606000001523>
- [10] A. Karadimitrakakis, A. L. Moustakas, and P. Vivo, "Large deviation approach to the outage optical mimo capacity," *CoRR*, vol. abs/1302.0614, 2013.

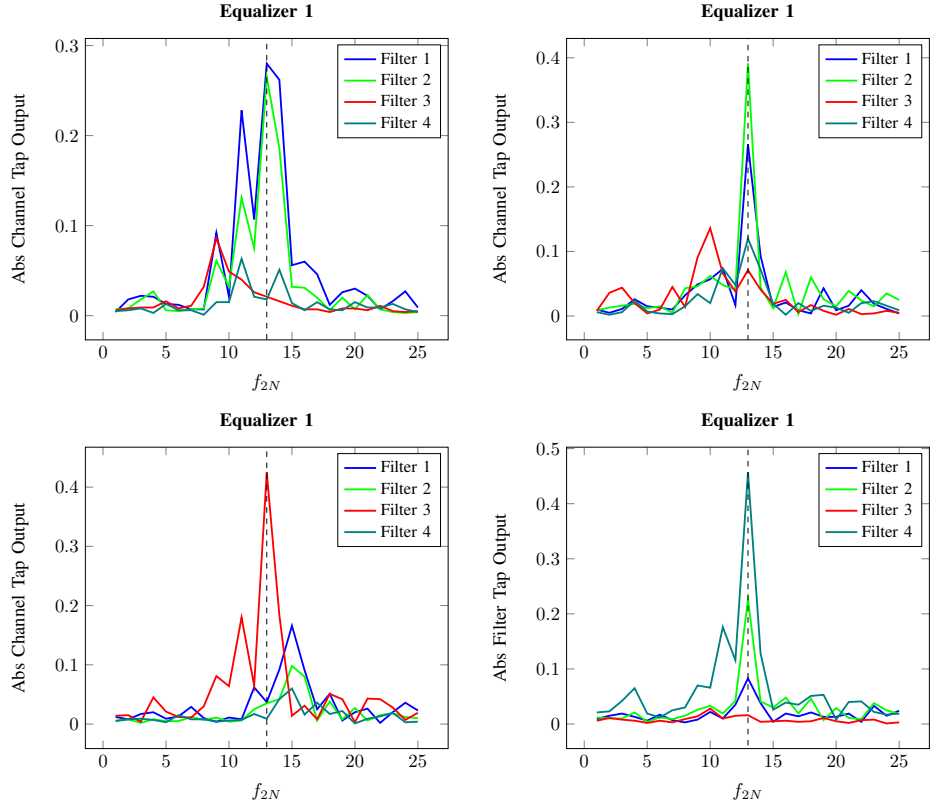


Fig. 5: Average value of the 500 different instantiations of the 4 filters for the 4 equalizers. The dashed line points the 13th tap.

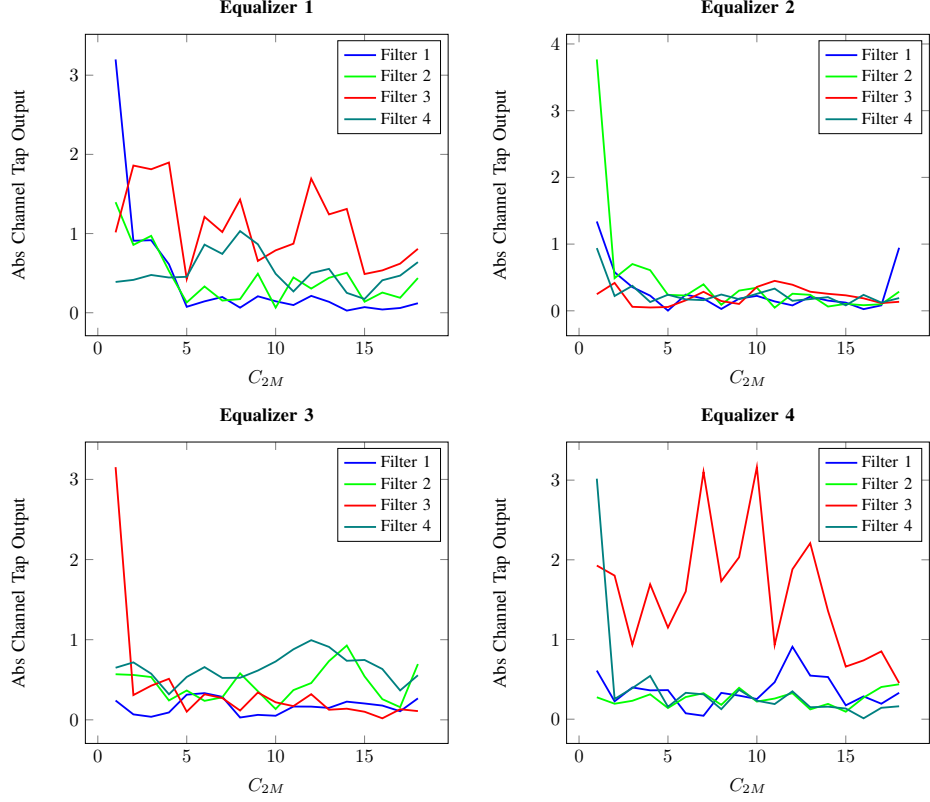


Fig. 6: Channel coefficients for the 4 equalizers.